

Control of atomic decay rates via manipulation of reservoir mode frequencies

I.E. Linington and B.M. Garraway

(Dated: November 5, 2018)

We analyse the problem of a two-level atom interacting with a time-dependent dissipative environment modelled by a bath of reservoir modes. In the model of this paper the principal features of the reservoir structure remain constant in time, but the microscopic structure does not. In the context of an atom in a leaky cavity this corresponds to a fixed cavity and a time-dependent external bath. In this situation we show that by chirping the reservoir modes sufficiently fast it is possible to inhibit, or dramatically enhance the decay of the atomic system, even though the gross reservoir structure is fixed. Thus it is possible to extract energy from a cavity-atom system faster than the empty cavity rate. Similar, but less dramatic effects are possible for moderate chirps where partial trapping of atomic population is also possible.

PACS numbers: 42.50.Ct, 03.65.Yz

I. INTRODUCTION

The decay of an excited atomic state is manifestly affected by its environment. This has been evident since studies began on the effect of cavities and conducting plates on spontaneous emission [1, 2, 3, 4]. The boundary conditions of nearby surfaces affect the electromagnetic mode density and, in the simplest treatment, the application of Fermi's golden rule shows that the spontaneous emission rate is modified. However, with the development of high-Q cavities in the microwave [5] and optical regime [6] it was possible to have an oscillatory exchange of energy between a single atom and a single cavity mode of electromagnetic (EM) radiation. In this regime a single quantum of EM energy may be involved and the atom may become entangled with the cavity. It is often desirable to control quantum systems of this kind, for example, to try and make a specific state of the cavity field (see e.g. [7]), or to make entanglement, or in more complex systems, to make photons on demand [8]. However, the effect of the environment is always there as decoherence, or dissipation, and it almost always acts to degrade the quantum phenomena in which we are interested.

In this paper we will look at a model example of what we might do in the environment to try and regain control. We will take the simplest quantum optical system of a two-level atom coupled to a leaky cavity. In our idealised system the cavity leaks through lossless dielectric mirrors, although there well may be other systems that fit the model such as coupled microwave cavities [9] or engineered reservoirs for ion traps [10]. For the optical cavity system, there are a number of well established types of quantum optical environment. For example, the thermal bath contains energy which ultimately leads to thermalisation of the atom and cavity. Rigged reservoirs [11] have bath states with coherence which add gain and noise to the field state. The broad-band squeezed vacuum [12] has correlations between different frequency bath states which in general has both the properties of a thermal bath and the presence of coherence. All of these environments would eventually excite an initially unexcited

atom in the cavity. The environment we will look at is one in which the bath, or reservoir modes, change their frequency as a function of time. This kind of environment would not excite an initially unexcited atom, although the dynamics of an initially excited atom would be affected. In general, we would expect that reservoir modes do have time-dependent properties, since they are themselves embedded in an uncontrolled environment. However, here we will suppose that we can at least control their frequency for a short period of time. The reservoir will be fully specified if the frequency and the strength of the coupling to the atom are known for each mode: this amounts to specifying the reservoir mode structure.

If we modulate all the reservoir mode frequencies by the same amount, keeping the coupling of each mode to the atom the same, the overall effect is the same as moving one of the cavity mirrors, which has been studied for the case of an oscillating mirror [13]. However, this case is also equivalent to a time-dependent detuning of the reservoir from the atomic transition frequency. This situation has been discussed in Ref. [14] where it was found that it was possible to inhibit the decay of the atom for particular modulation frequencies. Modulation of the phase of the atom-cavity coupling constant was also analysed by Agarwal [15] who showed that, for a low-Q cavity situation, the decoherence could be reduced with fast modulation. Temporal variation of both the phase and weight of the coupling strengths between an atom and a continuum, with variation of the atomic detuning was studied in Ref. [16]. In this case the bath modes had to be modulated identically and the time-dependence had to be a weak perturbation. However, it was shown that both enhancement and suppression of the decay rate relative to the golden rule limit is possible.

In this paper we aim to investigate a new and subtle case, where the mode frequencies and coupling constants are manipulated, but in such a way as to leave all macroscopic properties of the reservoir unaffected. The unaffected properties will be the overall spectral width and resonance frequency of the reservoir structure. To achieve this the bath modes both increase their frequency and change their coupling strength as shown in figure 1.

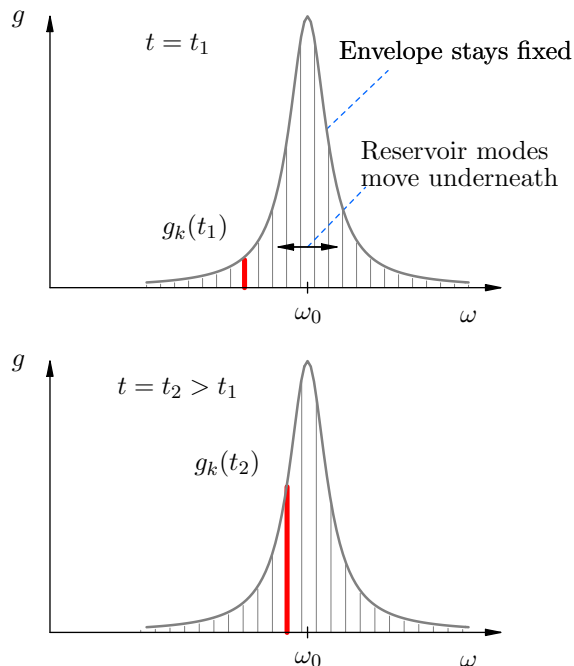


FIG. 1: Reservoir mode couplings $g_k(t)$ (see equation 1) at two different times t_1 and t_2 . The envelope of the couplings remains the same as the reservoir mode frequencies vary in time. Thus the coupling of the atom to an individual mode changes in time. The thick line indicates the same mode k at two different times, t_1 and t_2 . Since at time t_2 , this mode has moved to a different frequency under the static envelope, the coupling has changed accordingly.

Passing through the cavity resonance from below, the coupling strength of a mode to the atom first rises and then falls as the frequency is increased. The physical realisation could be a double cavity: one cavity couples to an atom and leaks to a second cavity which can have its end wall moved. We will discuss this realisation further in section V.

Without further analysis this situation would present us with a dilemma. The macroscopic structure of the atom-reservoir interaction is unchanged in time, but the individual bath modes only interact with the atom for a finite time. It may not be immediately clear that this situation can dramatically affect the atomic decay: at any point in time the atom has the same coupling to some bath modes. However, because the bath modes change, the history of the atom-bath interaction affects the time development of their population. We will find that in this case both enhanced and inhibited decay are possible.

The remainder of this paper is organised as follows. In section II we describe our model for the problem and derive the equations governing the dynamics of the atomic state populations. Section III reviews the standard problem of a two-level atom interacting with a high-Q cavity in the strong and weak coupling regimes. However, the section pays particular attention to the evolution of the

quantum state of the reservoir degrees of freedom, which are often traced over in similar calculations. Section IV summarises the main results of the investigation in the regimes of strong and weak coupling. Finally, in section V, we estimate the size of the effects that might be observed and summarise the findings of the paper.

II. DYNAMIC RESERVOIR MODEL

We consider a two-level atom, with states denoted $|0\rangle$ and $|1\rangle$, coupled to a reservoir of electromagnetic radiation modes at zero temperature. The reservoir modes, labelled by an index k , have *time-dependent* frequencies $\omega_k(t)$, and raising and lowering operators \hat{b}_k^\dagger and \hat{b}_k . The Hamiltonian for the evolution of the composite atom and reservoir system is given in the rotating wave approximation by ($\hbar = 1$)

$$\hat{H}(t) = \omega_0 \hat{\sigma}^+ \hat{\sigma}^- + \sum_k \omega_k(t) \left(\hat{b}_k^\dagger \hat{b}_k + 1/2 \right) + \sum_k g_k(t) \left(\hat{\sigma}^- \hat{b}_k^\dagger + \hat{b}_k \hat{\sigma}^+ \right), \quad (1)$$

where the atomic transition frequency is ω_0 , and $\hat{\sigma}^+ = |1\rangle\langle 0|$ and $\hat{\sigma}^- = |0\rangle\langle 1|$ are the atomic raising and lowering operators respectively. The electric dipole coupling of the k^{th} mode of the electromagnetic radiation field to the atomic transition $|0\rangle \leftrightarrow |1\rangle$ is denoted by $g_k(t)$. Without loss of generality, the $g_k(t)$ are chosen to be real. For simplicity, we will later choose the spectral profile of the coupling constants to be peaked at the frequency of the atomic transition. While the reservoir modes are redistributed, we will suppose that this envelope remains fixed. Therefore, the magnitude of the coupling constants $g_k(t)$ must vary in time to ensure this (see figure 1). We will also assume that whilst the frequency change of the reservoir modes may be very rapid from the point of view of the atom, it will not be so fast that it could create photons in the cavity by itself. In this sense the cavity field will adiabatically follow the motion of its end-mirror (see, e.g., Refs. [17, 18]).

To develop equations for the state vector we work in an interaction picture and so we may write the time-evolution operator as

$$\hat{U}(t, 0) = \exp \left(-i \int_0^t \sum_k \omega_k(\tau) \left(\hat{b}_k^\dagger \hat{b}_k + 1/2 \right) d\tau \right) \times \exp \left(-i \omega_0 t \hat{\sigma}^+ \hat{\sigma}^- \right) \hat{U}_I(t, 0). \quad (2)$$

The effect of the atom-reservoir interaction is contained in the term $\hat{U}_I(t, 0)$, which satisfies the Schrödinger equation

$$i \frac{d\hat{U}_I(t, 0)}{dt} = \hat{H}_I(t) \hat{U}_I(t, 0), \quad (3)$$

and the interaction picture Hamiltonian $\hat{H}_I(t)$ is given by

$$\begin{aligned} \hat{H}_I(t) = & \sum_k \left[g_k(t) \hat{\sigma}^- \hat{b}_k^\dagger \exp \left(i \int_0^t [\omega_k(\tau) - \omega_0] d\tau \right) \right. \\ & \left. + g_k(t) \hat{\sigma}^+ \hat{b}_k \exp \left(-i \int_0^t [\omega_k(\tau') - \omega_0] d\tau' \right) \right]. \end{aligned} \quad (4)$$

The state vector is expanded in terms of the eigenstates of the excitation number operator, $\hat{N} = \hat{\sigma}^+ \hat{\sigma}^- + \sum_k \hat{b}_k^\dagger \hat{b}_k$. Since \hat{N} commutes with the Hamiltonian (4), the number of quanta is a constant of the motion. For initial states we assume the system is prepared with the atom in its excited state, and the reservoir is initially empty, i.e. $|\psi(0)\rangle = |1\rangle \otimes |\dots 0\dots\rangle$. Then the state vector at time t may be written as

$$\begin{aligned} |\psi(t)\rangle = & \hat{U}_I(t, 0) |\psi(0)\rangle \\ = & c_a(t) |1\rangle \otimes |\dots 0\dots\rangle \\ & + \sum_k c_k(t) |0\rangle \otimes |\dots 1_k\dots\rangle \end{aligned} \quad (5)$$

where $c_a(t)$ is the amplitude for the atom to be found in its excited state, and $c_k(t)$ is the amplitude for the k^{th} mode of the reservoir to contain one excitation. Elimination of $\hat{H}_I(t)$ and $\hat{U}_I(t)$ from equations (3), (4) and (5) leads to the following coupled differential equations for the amplitudes $c_a(t)$ and $c_k(t)$:

$$i \frac{\partial c_a(t)}{\partial t} = \sum_k g_k(t) \exp \left(-i \int_0^t [\omega_k(\tau) - \omega_0] d\tau \right) c_k(t) \quad (6)$$

$$i \frac{\partial c_k(t)}{\partial t} = g_k(t) \exp \left(i \int_0^t [\omega_k(\tau) - \omega_0] d\tau \right) c_a(t). \quad (7)$$

We can now eliminate the amplitudes $c_k(t)$ by integrating equation (7) and substituting the result into equation (6). Thus we obtain the integro-differential equation for $c_a(t)$, i.e.

$$\begin{aligned} \frac{\partial c_a(t)}{\partial t} = & - \int_0^t dt' \sum_k g_k(t) g_k(t') \\ & \times \exp \left(-i \int_0^t [\omega_k(\tau) - \omega_0] d\tau \right) \\ & \times \exp \left(i \int_0^{t'} [\omega_k(\tau') - \omega_0] d\tau' \right) c_a(t'). \end{aligned} \quad (8)$$

For much of the following analysis we will work in the limit of a continuum of reservoir modes so that the sum in (8) is replaced by an integral over a continuous variable ω . Thus we make the identifications

$$\omega_k(t) \rightarrow \omega_R(\omega, t) \quad (9)$$

$$g_k(t) \rightarrow g(\omega, t) \quad (10)$$

where ω refers to the *initial* frequencies of the field modes. The function $\omega_R(\omega, t)$ represents, at time t , the frequency of a bath mode which had frequency ω at $t = 0$. Hence, we will have $\omega_R(\omega, 0) = \omega$. We also introduce the density of states $\rho(\omega)$ at time $t = 0$ and then equation (8) is replaced by

$$\begin{aligned} \frac{\partial c_a(t)}{\partial t} \approx & - \int_0^t dt' \int_{-\infty}^{\infty} d\omega \rho(\omega) g(\omega, t) g(\omega, t') \\ & \times \exp \left(-i \int_0^t [\omega_R(\omega, \tau) - \omega_0] d\tau \right) \\ & \times \exp \left(i \int_0^{t'} [\omega_R(\omega, \tau') - \omega_0] d\tau' \right) c_a(t'). \end{aligned} \quad (11)$$

In addition, in equation (11), we have extended the lower frequency limit from 0 to $-\infty$. However, for optical transitions, ($\omega_0 \sim 10^{15} \text{s}^{-1}$), the effects of this approximation are similar to others already made (for example the rotating-wave approximation, or the assumption of a two-level atom), and may be neglected.

Later, we will also examine an idealised time-dependent bath spectrum, which is in fact just the frequency dependent population of the reservoir modes. We define this spectrum by considering those modes k_Δ ($k_\Delta \in \{k\}$) which have frequencies that lie within $\Delta\omega$ of a given frequency ω at a time t . That is, we let

$$S(\omega, t) \approx \frac{1}{\Delta\omega} \sum_{k_\Delta} |c_{k_\Delta}(t)|^2. \quad (12)$$

In the continuum limit the number of modes k_Δ in the sum is approximately $\Delta\omega \rho(\omega)$, and since the c_k are expected to vary smoothly with k in this limit, we finally let

$$S(\omega, t) \rightarrow \rho(\omega) |c_{k_\Delta}(t)|^2, \quad (13)$$

which applies to a representative k_Δ . Equation (13) will serve as an operational definition of the bath spectrum.

We will now specify a model reservoir structure to be used in equation (11). For a simple cavity model, we can assume that the single time reservoir structure function $\rho(\omega) |g(\omega, t)|^2$ is a Lorentzian, with width γ , centred on the atomic transition frequency ω_0 , i.e.

$$\rho(\omega) |g(\omega, t)|^2 = \frac{D^2 \gamma / \pi}{\gamma^2 + (\omega_R(\omega, t) - \omega_0)^2}. \quad (14)$$

This describes the time-dependent coupling of a bath mode, initially at ω . However, it also describes the instantaneous coupling to the bath of modes at time t . Since the structure has no time dependence, apart from the time dependence of ω_R , the basic reservoir structure is constant in time, in this model. This is also clear from the weight D of the Lorentzian, which is defined through the relation

$$\int_{-\infty}^{\infty} \rho(\omega) |g(\omega, t)|^2 d\omega = D^2. \quad (15)$$

We can see that this integral is independent of time for the chosen form (14). In the static case, where $\rho(\omega)|g(\omega, t)|^2$ is not a function of time, the Lorentzian (14) is a common choice for the reservoir structure [19, 20] and the resulting dynamics have been well explored (see, for example, [21, 22]). In the weak coupling limit, the Lorentzian reservoir structure ensures exponential decay of atomic population. Of course, equation (11) does not feature $\rho(\omega)|g(\omega, t)|^2$, but the two-time product $\rho(\omega)g(\omega, t)g(\omega, t')$. However, as already mentioned, $g(\omega, t)$ may be chosen to be real. Therefore the two-time product follows immediately as

$$\begin{aligned} \rho(\omega)g(\omega, t)g(\omega, t') &= \frac{D^2\gamma}{\pi\sqrt{(\gamma^2 + (\omega_R(\omega, t) - \omega_0)^2)}} \\ &\quad \times \frac{1}{\sqrt{(\gamma^2 + (\omega_R(\omega, t') - \omega_0)^2)}}. \end{aligned} \quad (16)$$

To proceed with the analysis, a specific form for the time dependence of the modes must also be chosen. In this paper we choose a simple case where all the bath-mode frequencies increase linearly at the same rate, i.e. a linear chirp, for which

$$\omega_R(\omega, t) = \omega + \chi t. \quad (17)$$

Some motivation for this will be given in section V. If

we now substitute (17) and (16) into (11) we find

$$\begin{aligned} \frac{\partial c_a(t)}{\partial t} &= -\frac{D^2\gamma}{\pi} \int_0^t dt' \int_{-\infty}^{\infty} d\omega \frac{\exp[-i(\omega - \omega_0)t - i\chi t^2/2]}{\sqrt{(\gamma^2 + (\omega - \omega_0 + \chi t)^2)}} \\ &\quad \times \frac{\exp[i(\omega - \omega_0)t' + i\chi t'^2/2]}{\sqrt{(\gamma^2 + (\omega - \omega_0 + \chi t')^2)}} c_a(t') \\ &= -\int_0^t dt' K(t, t') c_a(t'), \end{aligned} \quad (18)$$

i.e. an integro-differential equation with the kernel given by

$$\begin{aligned} K(t, t') &= \frac{D^2\gamma}{\pi} \int_{-\infty}^{\infty} d\omega \frac{\exp[-i(\omega - \omega_0)t - i\chi t^2/2]}{\sqrt{(\gamma^2 + (\omega - \omega_0 + \chi t)^2)}} \\ &\quad \times \frac{\exp[i(\omega - \omega_0)t' + i\chi t'^2/2]}{\sqrt{(\gamma^2 + (\omega - \omega_0 + \chi t')^2)}}. \end{aligned} \quad (19)$$

We also note that if we change variables to $\tau = t - t'$, and $\Delta = \omega - \omega_0 + \chi(t + t')/2$, equation (18) can be expressed as

$$\frac{\partial c_a(t)}{\partial t} = -\frac{D^2\gamma}{\pi} \int_0^t d\tau \int_{-\infty}^{\infty} d\Delta \frac{e^{-i\Delta\tau} c_a(t - \tau)}{\sqrt{[\gamma^2 + (\Delta + \chi\tau/2)^2][\gamma^2 + (\Delta - \chi\tau/2)^2]}}. \quad (20)$$

III. EVOLUTION OF A STATIC RESERVOIR

We are investigating the effects of manipulating a reservoir of field modes which will interact with an atom. That is, the reservoir changes in time. However, it will be helpful to discuss first the behaviour of the static problem. Here, none of the reservoir mode frequencies vary with time ($\chi = 0$), so equation (18) simplifies to

$$\begin{aligned} \frac{\partial c_a(t)}{\partial t} &= -\frac{D^2\gamma}{\pi} \int_0^t dt' \int_{-\infty}^{\infty} d\omega \frac{e^{-i(\omega - \omega_0)(t - t')}}{\gamma^2 + (\omega - \omega_0)^2} c_a(t') \\ &= -D^2 \int_0^t e^{-\gamma(t - t')} c_a(t') dt' \\ &= -\int_0^t K_s(t, t') c_a(t') dt'. \end{aligned} \quad (21)$$

Equation (21) can, for example, be solved for the dynamics of the atom by means of Laplace transforms. We may also use the method of *pseudomodes* [21]. For this system

a pseudomode amplitude $\mathcal{B}(t)$ is defined as

$$\mathcal{B}(t) = -iDe^{-\gamma t} \int_0^t e^{\gamma t'} c_a(t') dt', \quad (22)$$

and will represent the dynamics of the field. The dynamics of $c_a(t)$ are then contained in the following two equations which can be exactly solved and represent equation (21) [21]:

$$\frac{\partial c_a(t)}{\partial t} = -iD\mathcal{B}(t) \quad (23)$$

$$\frac{\partial \mathcal{B}(t)}{\partial t} = -iDc_a(t) - \gamma\mathcal{B}(t). \quad (24)$$

If the frequency scale associated with the reversible dynamics of the atom-field coupling D exceeds that for irreversible decay γ , then there will be a resonant exchange of energy between atom and cavity (Rabi oscillations) as a photon emitted by the atom is repeatedly emitted and re-absorbed. This is the regime of *strong coupling*. We

note that in the weak coupling limit the decay of the *cavity field* is seen to be given by γ . To improve the clarity of later discussions, we will now analyse the dynamics separately in the strong-coupling and weak-coupling regimes.

A. Strong Coupling

In the regime of strong coupling to the static reservoir ($D \gg \gamma$), the exact solution to equations (23,24) can be written as

$$c_a(t) = e^{-\gamma t/2} \left[\cos(\Omega t/2) + \frac{\gamma}{\Omega} \sin(\Omega t/2) \right], \quad (25)$$

where [22]

$$\Omega = \sqrt{4D^2 - \gamma^2}. \quad (26)$$

The population of the excited atomic state then undergoes Rabi oscillations at angular frequency Ω ($\approx 2D$), under an envelope decaying at rate γ . The atomic decay at a rate γ is a feature of strong coupling to the cavity, $D > \gamma/2$ in equation (26), and the chosen reservoir structure (14).

For later comparison we will determine the bath spectrum $S(\omega, t)$ defined in equation (13). In principle this

can be found by inserting the solution (25) into equation (7) and integrating. The resulting expression for $S(\omega, t)$ is very complicated and here we will instead derive this spectrum in the strong coupling limit where $D \gg \gamma$. Thus we take the solution (25) to be approximated by

$$c_a(t) \approx e^{-\gamma t/2} \cos(\Omega t/2). \quad (27)$$

Substituting the expression into (7) and integrating (using $c_k(0) = 0$) gives

$$c_k(t) = \frac{g_k}{2} \left\{ \frac{\exp[i(\omega_k - \omega_0 - \Omega/2 + i\gamma/2)t] - 1}{\omega_k - \omega_0 - \Omega/2 + i\gamma/2} + \frac{\exp[i(\omega_k - \omega_0 + \Omega/2 + i\gamma/2)t] - 1}{\omega_k - \omega_0 + \Omega/2 + i\gamma/2} \right\}. \quad (28)$$

We now substitute (28) into the definition for the spectrum, equation (13), and obtain an expression for $S(\omega, t)$ which simplifies in this strong coupling limit. This is because $S(\omega, t)$ is small away from either $\omega \approx \omega_0$ or $\omega \approx \omega_0 \pm \Omega/2$. As a result, if we also use the replacement $\omega_k \rightarrow \omega$ and the reservoir structure function (14), the spectrum can be simplified to:

$$S(\omega, t) \approx \frac{\gamma/2}{2\pi \left[(\omega - \omega_0 - \Omega/2)^2 + (\gamma/2)^2 \right]} \left[1 + e^{-\gamma t} - 2e^{-\gamma t/2} \cos((\omega - \omega_0 - \Omega/2)t) \right] + \frac{\gamma/2}{2\pi \left[(\omega - \omega_0 + \Omega/2)^2 + (\gamma/2)^2 \right]} \left[1 + e^{-\gamma t} - 2e^{-\gamma t/2} \cos((\omega - \omega_0 + \Omega/2)t) \right] + \frac{\gamma}{\pi \left[(\omega - \omega_0)^2 + \gamma^2 \right]} e^{-\gamma t} \sin^2(\Omega t/2). \quad (29)$$

In the long time limit the atom has completely decayed and the initial energy is distributed in the bath as

$$S(\omega, t \rightarrow \infty) = \frac{1}{2\pi} \left[\frac{\gamma/2}{(\omega - \omega_0 - \Omega/2)^2 + (\gamma/2)^2} + \frac{\gamma/2}{(\omega - \omega_0 + \Omega/2)^2 + (\gamma/2)^2} \right]. \quad (30)$$

(See also Ref. [23].)

It is seen from equation (29) that the atom interacts with modes in the approximate range $\omega_0 - \Omega/2$ to $\omega_0 + \Omega/2$ (in the sense that only modes in this range become significantly changed via interaction with the atom). As the interaction progresses the reservoir mode occupation probabilities develop away from the atomic frequency ω_0 at $\omega_0 \pm \Omega/2$ (the vacuum Rabi-splitting, [24, 25]). For the *intermediate coupling case*, where the tails of the Lorentzians in equation (29) overlap, the population appears to move outwards (figure 2). However, equa-

tion (29) is still approximately valid. For this intermediate coupling the system does undergo Rabi oscillations, ($D > \gamma/2$), without the strong coupling condition $D \gg \gamma$ being satisfied. In this same regime we find that chirping the reservoir mode frequencies has interesting effects as we will see in the next section. This is because the occupied modes at frequencies less than ω_0 may be brought back into resonance with the atom through the reservoir frequency manipulation and thus affect $|c_a(t)|^2$ via equation (6).

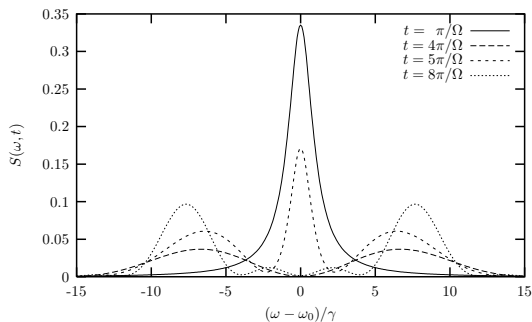


FIG. 2: Occupation of reservoir field-modes $S(\omega, t)$ at four different times. The times are chosen so that the atomic excited state probability, $|c_a(t)|^2$ is either zero ($t = \pi/\Omega, 5\pi/\Omega$), or at a local maximum ($t = 4\pi/\Omega, 8\pi/\Omega$). The reservoir is static ($\chi = 0$) and modes in the range $\omega_0 - \Omega/2$ to $\omega_0 + \Omega/2$ are occupied over the four Rabi cycles shown here. The parameter $D = 8\gamma$ (strong coupling). The calculation is based on the substitution of equation (25) into (7).

B. Weak Coupling

For reference later we note below the behaviour of the atomic dynamics in the weak coupling regime ($D \ll \gamma$). The exact solution to equations (23,24) shows damping at two different rates given approximately as D^2/γ and γ . The damping at rate γ only has a small effect at short times. An alternative approach notes that the kernel $K_s(t, t')$ in equation (21) is negligible away from $t' \approx t$. Then the coefficient $c_a(t')$ can only contribute to the integral at $t' \approx t$, so we may make the *Markov approximation*, and equation (21) simplifies to

$$\begin{aligned} \frac{\partial c_a(t)}{\partial t} &\approx -c_a(t) \int_0^t K_s(t, t') dt' \\ &\approx -\frac{\Gamma(t)}{2} c_a(t), \end{aligned} \quad (31)$$

where,

$$\Gamma(t) = \frac{2D^2}{\gamma} (1 - e^{-\gamma t}). \quad (32)$$

This time-dependent decay rate gives atomic dynamics which are correct to second order in $(D/\gamma)^2$ and approximates the short-time dynamics as well as the long time behaviour. For the latter, we see that the term $e^{-\gamma t}$ in $\Gamma(t)$ decreases rapidly over the decay-time of the atom, so we may then let

$$\Gamma(t) \approx \frac{2D^2}{\gamma}, \quad (33)$$

resulting in exponential time-dependence for the atom: $c_a(t) \approx \exp(-D^2 t/\gamma)$. The atom and reservoir become entangled and the amplitude $c_a(t)$ decays at a rate which is always less than the strong coupling case, equation (25).

IV. RESULTS FOR A TIME-DEPENDENT RESERVOIR

Exact, analytic solution of equation (18) has not proved possible. Square roots in the denominator introduce branch cuts in the complex angular frequency plane, and this creates difficulties in more than one approach. Therefore the solution to this problem must be numerical. However, in certain limits, an approximate analytical solution is possible, and the results are presented in sections IV A 1, IV A 3, and IV B.

Where a numerical solution for the amplitudes $c_a(t)$ and $c_k(t)$ has been required, it was obtained by integrating (6) and (7) for a discrete micro-bath of field modes, with the form (14) for the coupling constants, and linear chirp (17) for the time-dependence of the reservoir mode frequencies. The numerical method used was a fourth-order Runge-Kutta stepwise integration, with adaptive step size. A suitable density of states was chosen and the results were checked to make sure the dynamics of $|c_a(t)|^2$ and $|c_k(t)|^2$ were insensitive to this choice. (Typically about ten modes within one half-width γ of the reservoir structure function (14) was sufficient.) Results of this simulation were tested in the static ($\chi = 0$) case against the exact solution afforded by the method of pseudomodes (equation (25) and reference [21]), and for very high chirp rates against analytical predictions as discussed later in this paper (equation (40)).

A. Strong Coupling

The effects of reservoir chirp are examined in three regimes: low, intermediate and high chirp-rates. The classification depends on the rate of change of the mode frequencies χ [26], the time-scale of the atomic dynamics, and also the width of the occupied mode spectrum. As discussed in section III, even in the absence of frequency modulation, the time-scale of the atomic dynamics depends on ratio of the weight D to the width γ of the coupling spectrum. For strongly coupled systems ($D \gg \gamma$), the relevant time-scale is the Rabi period $2\pi/\Omega$, and since modes in the frequency range $\omega_0 - \Omega/2$ to $\omega_0 + \Omega/2$ interact significantly with the atom, a relevant parameter is the ratio of the frequency increase that each mode experiences during one Rabi period to the frequency range half-splitting $\Omega/2$. Thus we introduce

$$\xi = \frac{4\pi\chi}{\Omega^2} \quad (34)$$

as the parameter we will use to characterise the different types of behaviour. Then the specification of only two parameters in the model completely determines the dynamics: i.e. D/γ (the strength of the atom-cavity coupling) and the scaled chirp rate ξ . Within this parameter space, three categories of solution are found, as shown in figure 3. Here ‘low’ chirp corresponds to $\xi \ll 1$, ‘high’ chirp to $\xi \gg 1$, and all three categories will

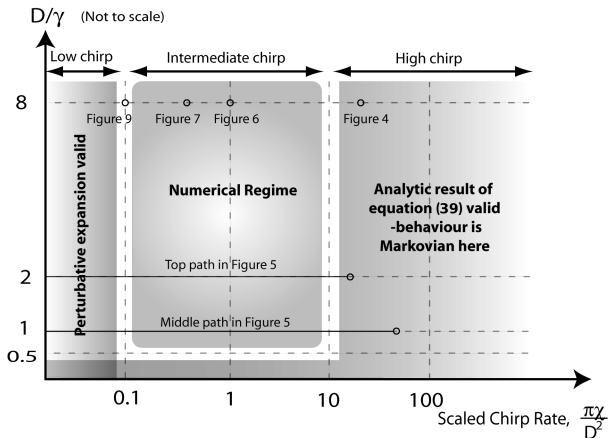


FIG. 3: Parameter space portrait highlighting the different character of solutions to equation (18) in different regions. The specific cases in figures 4-9 are indicated. The analytic result of equation (39) holds in the weak-coupling regime ($D < \gamma/2$), and also in the ‘high-chirp’ regime ($\xi \gg 1$), irrespective of D/γ .

be discussed separately below. Note that the definition of ξ only makes sense for strong coupling, $D > \gamma/2$, as this is the region in which Ω is real and non-zero (see equation (26)). However, in figure 3, to include both the strong and weak coupling regimes, we use $\pi\chi/D^2$ for the scaled chirp-rate, instead of ξ , above. For most of the plane shown, $\Omega \approx 2D$, and so this difference is minor.

1. High Chirp Rates

In the limit $\xi \gg 1$, each mode of the reservoir is effectively only coupled to the atom for a small fraction of one Rabi period. During this time, the occupation of a mode may increase slightly through equation (6), but does not grow large enough to re-populate the atomic excited state via equation (7). Therefore, although the atom-reservoir coupling is strong, Rabi oscillations are not observed. Manipulating the reservoir frequencies can change the *type* of atomic state behaviour from *non-Markovian* to *Markovian*. A specific example is shown in figure 4, which lies in the region of high chirp rate indicated on figure 3. In this case there is a dramatic difference in the evolution of the atomic population between the static reservoir (dashed oscillating curve) and the chirped reservoir (exponentially decaying curve).

To investigate this we note that when we chirp the mode frequencies at a high rate, the two-time product $\rho(\omega)g(\omega, t)g(\omega, t')$ of equation (16) is only non-negligible

when $t \approx t'$, i.e. the Lorentzians under the square-root separate when $\chi(t-t') \sim \gamma$. Making the Markov approximation, the integro-differential equation (18) becomes

$$\begin{aligned} \frac{\partial c_a(t)}{\partial t} &\approx -c_a(t) \frac{D^2\gamma}{\pi} \int_{-\infty}^{\infty} d\omega \frac{\exp[-i(\omega - \omega_0)t - \frac{i\chi}{2}t^2]}{\sqrt{(\gamma^2 + (\omega - \omega_0 + \chi t)^2)}} \\ &\quad \times \int_0^t dt' \frac{\exp[i(\omega - \omega_0)t' + \frac{i\chi}{2}t'^2]}{\sqrt{(\gamma^2 + (\omega - \omega_0 + \chi t')^2)}} \\ &\approx -c_a(t) \int_0^t dt' K(t, t') \\ &\approx -\frac{\Gamma(t)}{2} c_a(t), \end{aligned} \quad (35)$$

where we have defined a time-dependent decay rate as

$$\Gamma(t) = 2 \int_0^t K(t, t') dt'. \quad (36)$$

Time-dependent decay rates similar to $\Gamma(t)$ also arise in the time-convolutionless projection operator technique [27] in the second order approximation. We already encountered a similar time-dependent decay rate in the weakly coupled static reservoir in equation (32). The decay rate $\Gamma(t)$ tends to a constant value as $t \rightarrow \infty$, which corresponds to a Markovian limit. This limit is given by

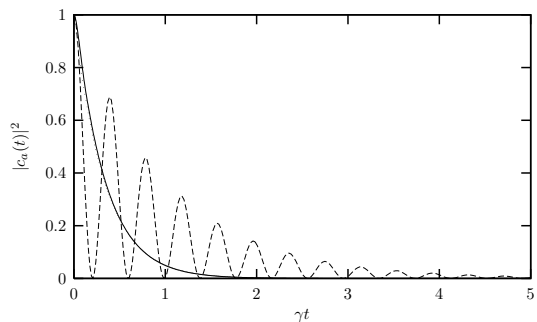


FIG. 4: Conversion from non-Markovian to Markovian dynamics by the introduction of reservoir chirp. In this example the dynamics were non-Markovian (dashed line) when the atom interacted with a static reservoir, as manifested by the Rabi oscillations. Chirp in the reservoir frequencies resulted in Markovian dynamics for the atom, and an exponential decay of $|c_a(t)|^2$ (solid line). The parameters used were $D = 8\gamma$ and for the chirped case, $\chi = 400\gamma^2$, which gives $\xi \approx 20$. Overlaid on the solid line (and nearly indistinguishable from it), is the analytic result of equations (39,40) (shown dotted) where $\Gamma_\infty \approx 3\gamma$.

$$\begin{aligned}
\Gamma_\infty &= \lim_{t \rightarrow \infty} \left\{ \Gamma(t) \right\} \\
&= \lim_{t \rightarrow \infty} \left\{ \frac{2D^2\gamma}{\pi} \int_0^t \int_{-\infty}^{\infty} \frac{\exp(i(\omega - \omega_0 + \chi t'/2)t')}{\sqrt{\gamma^2 + (\omega - \omega_0 + \chi t')^2}} \right. \\
&\quad \left. \times \frac{\exp(-i(\omega - \omega_0 + \chi t/2)t)}{\sqrt{\gamma^2 + (\omega - \omega_0 + \chi t)^2}} d\omega dt' \right\}. \tag{37}
\end{aligned}$$

To evaluate this we may change to variables $\Delta_d = \chi(t - t')/2$ and $\Delta = \omega - \omega_0 + \chi(t + t')/2$, so that

$$\begin{aligned}
\Gamma_\infty &= \frac{4D^2\gamma}{\pi\chi} \int_0^\infty d\Delta_d \int_{-\infty}^\infty d\Delta \frac{\exp(-2i\Delta\Delta_d/\chi)}{\sqrt{(\gamma^2 + (\Delta + \Delta_d)^2)(\gamma^2 + (\Delta - \Delta_d)^2)}} \\
&= \frac{2D^2\gamma}{\pi\chi} \int_{-\infty}^\infty d\Delta_d \int_{-\infty}^\infty d\Delta \frac{\exp(-2i\Delta\Delta_d/\chi)}{\sqrt{(\gamma^2 + (\Delta + \Delta_d)^2)(\gamma^2 + (\Delta - \Delta_d)^2)}}. \tag{38}
\end{aligned}$$

Then changing variables again, to $U = (\Delta + \Delta_d)/\gamma$ and $V = (\Delta - \Delta_d)/\gamma$, we finally obtain

$$\begin{aligned}
\Gamma_\infty &= \frac{D^2\gamma}{\pi\chi} \int_{-\infty}^\infty \frac{\exp\left(\frac{-iU^2\gamma^2}{2\chi}\right)}{\sqrt{(U^2 + 1)}} dU \int_{-\infty}^\infty \frac{\exp\left(\frac{iV^2\gamma^2}{2\chi}\right)}{\sqrt{(V^2 + 1)}} dV \\
&= \frac{D^2\gamma}{\pi\chi} K_0\left(\frac{i\gamma^2}{4\chi}\right) K_0\left(\frac{-i\gamma^2}{4\chi}\right). \tag{39}
\end{aligned}$$

Here K_0 is a modified Bessel function of zero order and Γ_∞ is necessarily real, since $K_0(z^*) = K_0(z)^*$. Further, we note that Γ_∞ is a monotonically decreasing function of χ . We will later argue that this expression for Γ_∞ is valid for $\xi \gg 1$ in the strong coupling case since the separation of the Lorentzians in equation (35), for which $\chi(t - t') \sim \gamma$, must take place on a time-scale shorter than the time-scale for the atomic dynamics. (This would be $1/D$ in the case of strong-coupling and no chirp.) With such high chirp, resonant modes which start to become occupied are moved far from resonance before they can act back on the atom, and are replaced by empty ones. In this way, the atom effectively sees an empty reservoir and obeys Markovian dynamics. A solution for the behaviour of $c_a(t)$ follows trivially:

$$c_a(t) \approx \exp(-\Gamma_\infty t/2). \tag{40}$$

Figure 5 shows the agreement between this approximate analytic result and a numerical simulation which used a bath of discrete field modes and did not make the Markov approximation. In fact, the result (40) also holds in the weak-coupling regime, independent of the rate χ , as discussed in sections IV B and V. For this reason as $\chi \rightarrow 0$ the static reservoir result $\Gamma_\infty = 2D^2/\gamma$, equation (33) is recovered. However, in the strong coupling case, this limit cannot be attained with equation (34), since, eventually, the constraint $\xi \gg 1$ is violated. In addition, we know that for $\chi = 0$ we should find the static decay

result γ implied by equation (25). Nevertheless, since $2D^2/\gamma > \gamma$ in the strong coupling regime, it is straightforward to have an *enhanced* decay rate (i.e. $\Gamma_\infty > \gamma$) if ξ is greater than unity, but not too high. In figure 5 we can find this for the low chirp part of the $D = 2\gamma$ curve ($12 \lesssim \chi/\gamma^2 \lesssim 38$), since only then is $\Gamma_\infty/\gamma > 1$ (with $\xi \gg 1$); for the rest of the curve the decay is *inhibited* relative to $\chi = 0$. However, if D/γ is even modestly increased the region of enhanced decay is increased substantially. It is interesting to note the equation (39) can be re-written as

$$\Gamma_\infty/\gamma = 2(D/\gamma)^2 \cdot \left[\frac{2|K_0(i/x)|^2}{\pi x} \right], \tag{41}$$

where $x = 4\chi/\gamma^2$. In this expression the inequality $2|K_0(i/x)|^2/\pi x \leq 1$ holds, with equality as x (i.e. χ) tends to zero. Since the factor D/γ is always greater than unity for strong coupling, we may have either *enhanced* or *inhibited* Markovian decay, depending on the value of χ . Equation (41) can also be used to motivate the constraint $\xi \gg 1$ introduced above. Since the time-scale t_{at} for atomic dynamics is now $1/\Gamma_\infty$, and the factor $2|K_0(i/x)|^2/\pi x$ is always less than (or equal to) unity, it follows that $t_{at} \geq \gamma/2D^2$. Since the time-width of the kernel is approximately γ/χ , the system will be Markovian if $\gamma/\chi \ll t_{at}$. Since $\xi \sim \pi\chi/D^2$ for $D > \gamma$, this will always be true if $\xi \gg 2\pi$.

For very large chirp, compared to γ^2 , we can expand the Bessel functions in equation (39) to obtain the approximate result

$$\Gamma_\infty/\gamma \rightarrow \left(\frac{D}{\gamma}\right)^2 \cdot \frac{\gamma^2}{\pi\chi} [\ln(4\chi/\gamma^2)]^2, \tag{42}$$

which slowly decreases as χ/γ^2 is increased.

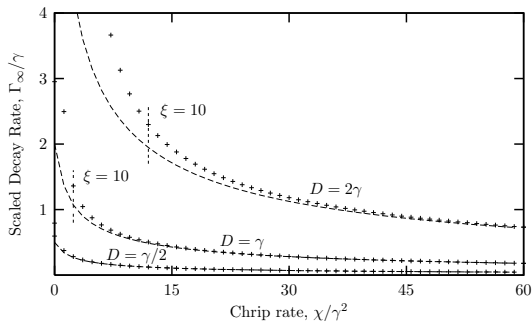


FIG. 5: Dependence of decay rate Γ_∞ on the chirp-rate χ . The dashed lines show the prediction of equation (39), whereas the crosses show the decay rates extracted from numerical solution (without making the Markov approximation) by fitting an exponential decay to the data. The parameters used for the three curves were $D = \gamma/2, \gamma$, and 2γ . Note that the fit is only expected to be good for $\xi \gg 1$, since for smaller chirp-rates than this, the behaviour of $|c_a(t)|^2$ is not necessarily an exponential decay and may even be oscillatory. Thus for the highest two values of D the position of $\xi = 10$ is marked. The chirp χ enhances the decay when $\Gamma_\infty/\gamma > 1$.

2. Intermediate Chirp Rates

As already discussed in section III A, in the static case the excitation of the reservoir modes moves outwards from ω_0 over several Rabi cycles towards final peaks at $\omega_0 \pm \Omega/2$. Now in the intermediate-chirp case, the frequency of the modes is increased by approximately the same amount over one Rabi-cycle. That is, the occupied modes are brought back into resonance with the atom on every Rabi-cycle. This can have a profound effect on the dynamics of the atomic excited state probability, $|c_a(t)|^2$, since occupied modes with angular frequency in the vicinity of ω_0 have the strongest interaction with the atom, as can be seen from equation (6).

In this regime of intermediate chirp rate ($\xi \sim 1$) and strong coupling ($D \gg \gamma$), we must rely on numerical results. As illustrated in figure 3, two free parameters, i.e. D/γ and the rate of redistribution of reservoir mode frequencies, label the dynamics of the system. A numerical search was conducted over this plane, and it was found that Rabi oscillations were inhibited over most of this region. The explanation for this is that occupied modes of the reservoir are moved from resonance before they have a chance to re-populate the atom. A typical example is shown in figure 6. Additionally, for $D/\gamma \lesssim 15$, there is a particular chirp-rate for which a ‘recycling condition’ is fulfilled and the vacuum Rabi-splitting in the reservoir doesn’t occur. A significant population may become trapped in a cycle of resonant exchange between atom and reservoir, and Rabi oscillations may persist for much longer than in the static case. The atomic behaviour is shown in figure 7. We also note that the oscillation frequency increases with increasing chirp-rate as is seen empirically from simulations. In figure 8 we see the corresponding spectrum of excitation in the reservoir for two

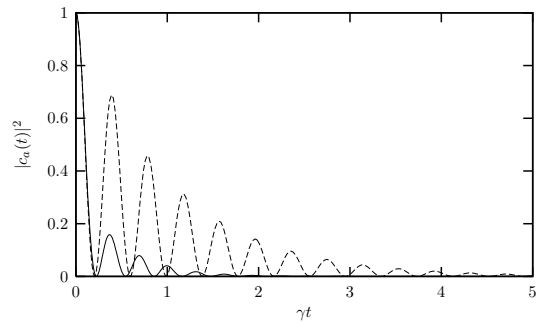


FIG. 6: Figure showing enhanced decay of the envelope of $|c_a(t)|^2$ caused by manipulation of the reservoir modes to which the atom is coupled (by a linear chirp). We note that the Rabi period is modified by manipulation of the reservoir mode frequencies. Parameters are $D = 8\gamma$ and for the solid line, $\chi = 20\gamma^2$. Thus $\xi \approx 1.0$. For comparison, the dashed line shows $|c_a(t)|^2$ for the case with no chirp ($\chi = 0$).

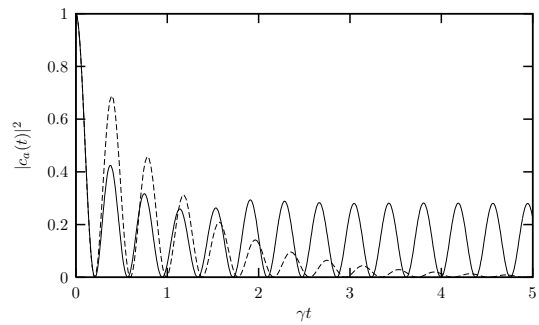


FIG. 7: Inhibition of decay and trapping of population with a chirped reservoir. The parameters are $D = 8\gamma$ and for the solid line, $\chi = 8.4\gamma^2$ (which implies $\xi \approx 0.42$). For comparison, the dashed line shows $|c_a(t)|^2$ for the case with no chirp ($\chi = 0$).

pairs of times. In each case the structured peak at higher frequencies is sufficiently detuned for this reservoir population to be effectively decoupled from the atomic dynamics. Therefore, excitation simply moves to higher frequencies at later times, as may be seen by comparing the spectra after 10 and 20 Rabi cycles. This non-interacting peak has an area of approximately a half, which represents the population that was ‘pushed’ to frequencies above ω_0 during the Rabi splitting at early times. We see that the left hand peak, which is centred at the atomic transition, remains on resonance as individual mode frequencies pass through this region. It does invert periodically during the time evolution, but this population exchange, or recycling, between the atom and *locally resonant* reservoir modes is very stable. For example, we can see that at the same part of the cycle the shape of this peak is relatively unchanged between (a) and (c) [and between (b) and (d)] in figure 8. This behaviour is quite different to that seen for the static reservoir in figure 2.

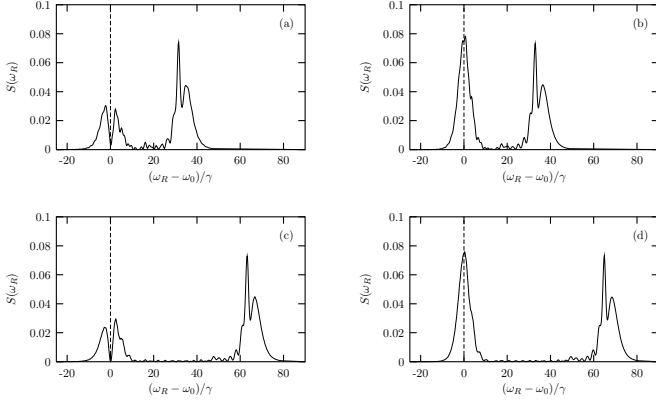


FIG. 8: The reservoir excitation spectrum during the stable oscillations of figure 7. The horizontal axis shows the scaled time-dependent detuning from the atomic transition frequency (vertical dashed line), where $\omega_R = \omega + \chi t$. For (a-d) $\gamma t \sim 3.81, 4.00, 7.60, 7.79$, and other parameters are as for figure 7, i.e. $D = 8\gamma, \chi = 8.4\gamma^2$. The times selected correspond to approximately: (a) 10; (b) 10.5; (c) 20; and (d) 20.5 Rabi oscillations.

3. Low Chirp Rates

In the regime of strong coupling and very low chirp ($\xi \ll 1$) the basic behaviour of the system will be to perform Rabi oscillations of the type found in equation (25). The weak chirp will be expected to perturb the dynamics only slightly. In the example shown in figure 9 the difference between the chirped and unchirped dynamics is very small, although it may be noticed the the chirped bath results in a slightly raised Rabi frequency. This frequency shift might be observable if the decay rate is low enough that a large phase shift accumulates in the Rabi oscillations. To evaluate the size of this effect we examine a perturbative solution found by expanding the denominator of equation (20) in powers of χ . Thus, for the kernel of equation (20)

$$K(\tau) = \frac{D^2\gamma}{\pi} \int_{-\infty}^{\infty} d\Delta \frac{\exp(-i\Delta\tau)}{\sqrt{[\gamma^2 + (\Delta + \chi\tau/2)^2][\gamma^2 + (\Delta - \chi\tau/2)^2]}}$$

$$\sim \frac{D^2\gamma}{\pi} \int_{-\infty}^{\infty} d\Delta \frac{e^{-i\Delta\tau}}{\gamma^2 + \Delta^2} \left[1 - \frac{\chi^2\tau^2}{4} \frac{\gamma^2 - \Delta^2}{(\gamma^2 + \Delta^2)^2} + \dots \right], \quad (43)$$

to order χ^2 . The method of pseudomodes (see section III and Ref. [21]) could be used to analyse this kind of kernel structure, but here we will simply examine the Laplace transform of equation (20) to find the perturbation of the Rabi frequency. To do this we first perform the integral over the detuning Δ in equation (43) so that with the approximate kernel (and given $\tau > 0$)

$$K(\tau) = D^2 e^{-\gamma\tau} \left[1 - \frac{\chi^2\tau^2}{16\gamma^2} (1 + \gamma\tau + (\gamma\tau)^2) \right]. \quad (44)$$

If we Laplace transform equation (20) and solve for $\tilde{c}_a(s)$, the transform of $c_a(t)$, we find

$$\tilde{c}_a(s) = \frac{1}{s + \tilde{K}(s)}, \quad (45)$$

where $\tilde{K}(s)$ is the transform of equation (43) and we let $c_a(0) = 1$. Using the approximate kernel (44) we will find that

$$\tilde{K}(s) = \frac{D^2}{s + \gamma} \left[1 - \frac{\chi^2}{8\gamma^2(s + \gamma)^2} - \frac{3\chi^2}{8\gamma(s + \gamma)^3} - \frac{3\chi^2}{2(s + \gamma)^4} \right]. \quad (46)$$

If we momentarily set χ to zero we see that, if we substitute equation (46) into equation (45), the poles in the right hand side of equation (45) are located at $s = -\gamma/2 \pm i\Omega/2$, where Ω is given in equation (26). This represents the damped oscillations of equation (25). If we now admit a finite value of χ , we seek the perturbed locations of the poles in the approximate form

$$s = -\frac{\gamma}{2} \pm i\frac{\Omega}{2} + \delta\chi^2. \quad (47)$$

The factor δ is found by substitution into the equation $s + \tilde{K}(s) = 0$. Since the modification of the decay rate is small, and not of interest, we examine the imaginary part of δ to find that $\text{Im}(\delta) \sim \pm 1/(8\Omega\gamma^2)$ and then the new Rabi frequency Ω' is approximately

$$\Omega' \sim \Omega \left(1 + \frac{\chi^2}{4\Omega^2\gamma^2} \right). \quad (48)$$

In the above we also used the strong coupling approximation ($D, \Omega \gg \gamma$). Even if the correction to the Rabi frequency is small, the effect may be noticeable since there will be an accumulated phase shift over time. Since the largest usable time in this limit is of order $1/\gamma$, it follows that the largest phase difference is approximately given

by

$$\Delta\Phi = (\Omega' - \Omega)T \sim \left(\frac{\chi^2}{4\Omega^2\gamma^2} \right) \left(\frac{\Omega}{\gamma} \right). \quad (49)$$

Thus even if the first term in brackets is small, since it is the correction to the Rabi frequency in equation (48), the strong coupling regime ensures the second term is large and so the resulting phase difference may be of a reasonable size. Note that the effect will be made more visible, not only by increasing the chirp χ , but also by *reducing* the strong atom-cavity coupling.

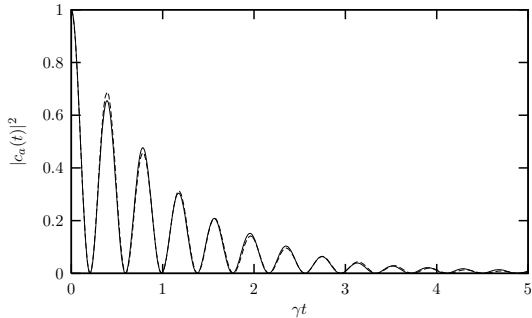


FIG. 9: For low chirp-rates, the atom experiences coupling to the same set of modes for several Rabi cycles and, consequently, the effects of the chirp are small. Parameters chosen were $D = 8\gamma$, and for the solid line, $\chi = 2\gamma^2$, which corresponds to $\xi \approx 0.1$. For comparison, the dashed line shows $|c_a(t)|^2$ for the case with no chirp ($\chi = 0$).

B. Weak Coupling

In the limit $D \ll \gamma$, the behaviour of $|c_a(t)|^2$ is Markovian. This remains true, irrespective of how the reservoir mode frequencies are manipulated. Therefore, for weakly-coupled reservoirs, the analysis of section IV A 1, culminating in equation (40), is valid for all chirp-rates. The region of weak coupling corresponds to the horizontal strip at the bottom of figure 3. Note that the expansion [28]

$$\lim_{|z| \rightarrow \infty} \{K_0(z)\} \sim \sqrt{\frac{\pi}{2z}} e^{-z} \left(1 - \frac{1}{8z} + \frac{9}{128z^2} + \dots \right) \quad (50)$$

implies that the decay constant Γ_∞ tends to the result of the static reservoir, equation (33), in the low-chirp limit, as it should. We can also find the leading correction, so that as $\chi \rightarrow 0$

$$\Gamma_\infty \rightarrow \frac{2D^2}{\gamma} \left(1 - \frac{2\chi^2}{\gamma^4} + \dots \right). \quad (51)$$

V. CONCLUSION

We have investigated the effects on the dynamics of an open quantum system of a particular manipulation of

the reservoir mode frequencies. While other authors have discussed reservoirs with time-dependent properties, we have here considered the subtle case where all *macroscopic* properties of the reservoir remain *static*, while the microscopic structure of the reservoir changes. This problem is intriguing, since the effects are non-trivial, and cannot easily be guessed in advance. It is tempting to think that since the only difference with the usual, static case is a redistribution of reservoir mode *populations*, only non-Markovian systems would be affected. This is not the case, however, and an effect can be seen for both Markovian and non-Markovian systems.

We have characterised the nature of the dynamics in three different regions of parameter space (see figure 3) and found conditions for each type of behaviour in section IV. It is shown that manipulation of the reservoir mode frequencies may alter the *nature* of the dynamics (from non-Markovian to Markovian behaviour) when the chirp-rate is high ($\xi \gg 1$). Analytical results are presented for the decay in this case (equations (39) and (40)). The resulting decay may be enhanced or inhibited, compared to the un-chirped case. In the case of strong coupling and low chirp, the chirp manifests itself as a frequency shift in the Rabi oscillations (equation (48)).

In order to realise the effects of section IV in the context of optical cavity QED it would be necessary to construct a high-Q cavity and a reservoir whose mode frequencies could be manipulated as described above, i.e. without altering the envelope of the coupling constants near the atomic resonance. Ideally, if the resonant frequency of the cavity is to remain unchanged (at $\omega_0/2\pi$), its cavity mirrors must be fixed, too. Since there will be losses through the cavity mirrors, i.e. a coupling to the external environment, the bath mode frequencies may be altered by changing the properties of that external environment. This would be sufficient to isolate the basic effect from, for example, changing the position of the cavity resonance (as in Ref. [13]). The most simple way of doing this would be to have an inner and outer cavity, with lengths ℓ and L . We can suppose that the outer mirror can be moved by a piezoelectric actuator, or similar device, which will change the length L . Then for small fractional changes in the outer cavity length we can write

$$\frac{\partial\omega}{\partial t} \approx -\frac{\omega}{L} \frac{\partial L}{\partial t} \approx -\frac{\omega_0}{L} \frac{\partial L}{\partial t}, \quad (52)$$

so that

$$\chi \approx -\frac{\omega_0}{L} \frac{\partial L}{\partial t}. \quad (53)$$

To illustrate the potential size of any observable effects, we consider some specific cases. First we take an optical atomic transition with angular frequency $\omega_0/2\pi \sim 3.5 \times 10^{14}$ Hz and a $40 \mu\text{m}$ inner cavity for which $\gamma/2\pi \sim 4.1$ MHz and $D/2\pi \sim 34$ MHz [25, 29]. This is in the strong coupling regime. For the outer cavity we let $L = 1\text{cm}$, and we assume here that the inner cavity is diffractively coupled to the outer cavity to enhance

the mode density, whilst maintaining a strong directional property. If we can move the out-most mirror at a speed of 0.1 ms^{-1} for the short time necessary, we find that $\chi \sim 2.2 \times 10^{16} \text{ s}^{-2}$. Then $\xi \approx 1.52$, which is enough to enter the intermediate chirp region indicated in figure 3 and discussed in section IV A 2. If we would increase the mirror speed to 0.65 ms^{-1} , ξ increases to approximately ten, which places us in the high chirp, strong coupling regime of figure 3. In this case equation (39) applies and we obtain an enhancement of decay: $\Gamma_\infty/\gamma = 5.05$. This enhanced decay can be increased even further if, for example, the cavity decay rate is reduced by a factor of ten: in that case $\Gamma_\infty/\gamma = 13.6$. As an example of inhibited decay we can simply reduce D so that $D \ll \gamma$. In this case we are in the weak coupling regime and the inhibition of decay relative to the static reservoir case is independent of D and given by a factor of approximately

$$\frac{\Gamma_\infty}{(2D^2/\gamma)} \approx 9.92 \times 10^{-4}, \quad (54)$$

when $\gamma/2\pi \sim 0.41 \text{ MHz}$ and the speed is 0.65 ms^{-1} , as

above.

We have seen that many of the effects described here could be tested with currently available experimental parameters. For an atom weakly coupled to a high-Q cavity, the inhibition of decay and decoherence is considerable, with the possibility of suppressing the decay rate by a factor of 10^3 . In the case of strong coupling, atomic decay can be inhibited (for high chirp χ) or enhanced. The examples given show an enhancement of decay by a factor of 5 or 14. This factor can be increased if the ratio D/γ is increased along with the smallest cavity chirp consistent with $\xi \gg 1$. An attractive feature of this model is that the suppression, or enhancement, could be turned on and off at will by moving or not moving the mirror of an *outer* cavity. In the case of enhanced decay, this means that the controlled motion of an outer cavity mirror can extract energy from the inner cavity-atom system.

This work was supported in part by the UK Engineering and Physical Sciences Research Council.

-
- [1] E.M. Purcell, Phys. Rev. **69**, 681 (1946).
[2] D. Kleppner, Phys. Rev. Lett. **47**, 233 (1981).
[3] P. Goy, J.M. Raimond, M. Gross, and S. Haroche, Phys. Rev. Lett. **50**, 1903 (1983).
[4] W. Jhe, A. Anderson, E.A. Hinds, D. Meschede, L. Moi, and S. Haroche, Phys. Rev. Lett. **58**, 666 (1986).
[5] D. Meschede, H. Walther, and G. Müller, Phys. Rev. Lett. **54**, 551 (1985).
[6] R.J. Thompson, G. Rempe, and H.J. Kimble, Phys. Rev. Lett. **68**, 1132 (1992).
[7] M. Weidinger, B.T.H. Varcoe, R. Heerlein, and H. Walther, Phys. Rev. Lett. **82**, 3795 (1999); B.T.H. Varcoe, S. Brattke, M. Weidinger, H. Walther Nature **403**, 743 (2000).
[8] See, for example: B. Lounis and M. Orrit, Rep. Prog. Phys. **68**, 1129 (2005); M. Keller, B. Lange, K. Hayasaka, W. Lange, and H. Walther, Nature **431**, 1075 (2004).
[9] J.M. Raimond, M. Brune, and S. Haroche, Phys. Rev. Lett. **79**, 1964 (1997).
[10] C.J. Myatt, B.E. King, Q.A. Turchette, C.A. Sackett, D. Kielpinski, W.M. Itano, C. Monroe, and D.J. Wineland, Nature **403**, 269 (2000); Q.A. Turchette, C.J. Myatt, B.E. King, C.A. Sackett, D. Kielpinski, W.M. Itano, C. Monroe, and D.J. Wineland, Phys. Rev. A **62**, 053807 (2000).
[11] M.A. Dupertuis and S. Stenholm, J. Opt. Soc. Am. **B4** 1094 (1987).
[12] See, for example, B.J. Dalton, Z. Ficek, and S. Swain, J. Mod. Opt. **46**, 379 (1999).
[13] C.K. Law, S.-Y. Zhu, and M.S. Zubairy, Phys. Rev. A **52**, 4095 (1995).
[14] M. Janowicz, Phys. Rev. A **61**, 025802 (2000).
[15] G.S. Agarwal, Phys. Rev. A **61**, 013809 (2000).
[16] A.G. Kofman and G. Kurizki, Phys. Rev. Lett. **87**, 270405 (2001).
[17] M. Janowicz, Phys. Rev. A **57**, 4784 (1998).
[18] V.V. Dodonov and A.B. Klimov, Phys. Rev. A **53**, 2664 (1996).
[19] S.M. Barnett and P.M. Radmore, *Methods in Theoretical Quantum Optics*, Oxford Series on Optical and Imaging Sciences (Oxford University Press, 1997).
[20] R. Lang, M.O. Scully, and W.E. Lamb, Jr., Phys. Rev. A **7**, 1788 (1973).
[21] B.M. Garraway, Phys. Rev. A **55**, 2290 (1997); Phys. Rev. A **55**, 4636 (1997).
[22] P. Lambropoulos, G.M. Nikolopoulos, T.R. Nielsen, and S. Bay, Rep. Prog. Phys. **63**, 455 (2000).
[23] H.J. Carmichael, R.J. Brecha, M.G. Raizen, H.J. Kimble and P.R. Rice Phys. Rev. A **40**, 5516 (1989).
[24] J.J. Sanchez-Mondragon, N.B. Narozhny, and J.H. Eberly, Phys. Rev. Lett. **51**, 550 (1983).
[25] A. Boca, R. Miller, K.M. Birnbaum, A.D. Boozer, J. McKeever, and H.J. Kimble, Phys. Rev. Lett. **93**, 233603 (2004).
[26] After a time t each mode increases its frequency by χt , see (17).
[27] F. Shibata, Y. Takahashi and H. Hashitsuma, J. Stat. Phys. **17**, 171 (1977); W.T. Strunz and T. Yu, Phys. Rev. A **69**, 052115 (2004); H.-P. Breuer, B. Kappler and F. Petruccione, Ann. Phys. (NY) **291**, 36 (2001).
[28] L.S. Gradshteyn and I.M. Ryzik, *Table of Integrals, Series and Products*, (Academic Press, 2000).
[29] R. Miller, T.E. Northup, K.M. Birnbaum, A. Boca, A.D. Boozer, and H.J. Kimble, J. Phys. B: At. Mol. Opt. Phys. **38**, S551 (2005).